

# GPIb $\alpha$ CAAR T cells function like a Trojan horse to eliminate autoreactive B cells to treat immune thrombocytopenia

Jie Zhou,<sup>1,2\*</sup> Yanyan Xu,<sup>3\*</sup> Jinhui Shu,<sup>1,2</sup> Haojie Jiang,<sup>3</sup> Linlin Huang,<sup>1,2</sup> Min Xu,<sup>1,2</sup> Junling Liu,<sup>3</sup> Yu Hu,<sup>1,2</sup> and Heng Mei<sup>1,2</sup>

<sup>1</sup>Institute of Hematology, Union Hospital, Tongji Medical College, Huazhong University of Science and Technology, Wuhan, Hubei; <sup>2</sup>Hubei Clinical Medical Center of Cell Therapy for Neoplastic Disease, Wuhan, Hubei and <sup>3</sup>Department of Biochemistry and Molecular Cell Biology, Shanghai Jiao Tong University School of Medicine, Shanghai, China

\*JZ and YX contributed equally as first authors.

**Correspondence:** H. Mei  
hmei@hust.edu.cn

Y. Hu  
dr\_huyu@126.com

**Received:** July 2, 2023.

**Accepted:** January 23, 2024.

**Early view:** February 1, 2024.

<https://doi.org/10.3324/haematol.2023.283874>

©2024 Ferrata Storti Foundation

Published under a CC BY-NC license



## Abstract

Breakthrough treatment for refractory and relapsed immune thrombocytopenia (ITP) patients is urgently needed. Autoantibody-mediated platelet clearance and megakaryocyte dysfunction are important pathogenic mediators of ITP. Glycoprotein (GP) Ib $\alpha$  is a significant autoantigen found in ITP patients and is associated with poor response to standard immunosuppressive treatments. Here, we engineered human T cells to express a chimeric autoantibody receptor (CAAR) with GPIb $\alpha$  constructed into the ligand-binding domain fused to the CD8 transmembrane domain and CD3 $\zeta$ -4-1BB signaling domains. We performed cytotoxicity assays to assess GPIb $\alpha$  CAAR T-cell selective cytolysis of cells expressing anti-GPIb $\alpha$  B-cell receptors *in vitro*. Furthermore, we demonstrated the potential of GPIb $\alpha$  CAAR T cells to persist and precisely eliminate GPIb $\alpha$ -specific B cells *in vivo*. In summary, we present a proof of concept for CAAR T-cell therapy to eradicate autoimmune B cells while sparing healthy B cells with GPIb $\alpha$  CAAR T cells that function like a Trojan horse. GPIb $\alpha$  CAAR T-cell therapy is a promising treatment for refractory and relapsed ITP patients.

## Introduction

Primary immune thrombocytopenia (ITP) is a bleeding disorder mainly mediated by pathogenic anti-platelet autoantibodies secreted by autoreactive B cells and plasma cells, eventually leading to accelerated platelet destruction and megakaryocyte dysfunction.<sup>1-3</sup> Platelet autoantibodies are predominantly directed against the platelet glycoproteins (GP) IIb/IIIa (CD41/CD61) and GPIb/IX (CD42b/CD42c/CD42a) in ITP.<sup>4,5</sup> B-cell-targeted therapies in ITP patients appear to be well tolerated short term but lack long-term tolerance, and many patients relapse after drug withdrawal. Only 20% to 30% of patients treated with CD20-targeted B-cell depletion therapy (rituximab) can achieve a long-term response (5 years).<sup>6-8</sup> A possible reason for this therapeutic failure is the presence of rituximab-resistant splenic memory B cells and long-lived plasma cells (LLPC) secreting high-affinity autoantibodies.<sup>9-12</sup> Failure of splenectomy therapy may be due to the presence of peripheral memory B cells and bone marrow LLPC in ITP patients.<sup>9,13</sup> Thus, novel therapeutic strategies that eradicate autoreactive B cells (including

memory B cells) while sparing healthy B cells would significantly advance ITP treatment.

Chimeric antigen receptor (CAR) T-cell therapy has achieved remarkable success in neoplastic hematologic disorders, especially B-cell malignancies, with the cost of eradicating normal B cells. Based on CAR T-cell therapy, the concept of chimeric autoantibody receptor T cells (CAAR T) was proposed and applied to the treatment of pemphigus<sup>14</sup> and muscle-specific tyrosine kinase myasthenia gravis.<sup>15</sup> The extracellular ligand-binding domain of the CAAR structure was designed to contain autoantigens, thus mediating the specific cytolysis of autoreactive B cells by T cells in the above studies.

GPIb $\alpha$ , a surface membrane protein of platelets, initiates signaling events within platelets by binding to the A1 domain of von Willebrand factor (VWF).<sup>16,17</sup> In ITP, platelet-associated anti-GPIb/IX antibodies are associated with a lower platelet count<sup>18,19</sup> and inadequate responses to corticosteroids, intravenous immunoglobulin (IVIg), rituximab, and recombinant human thrombopoietin (rhTPO) compared with anti-GPIIb/IIIa antibodies.<sup>20-24</sup> Epitope mapping of ITP

sera containing anti-GPIb/IX antibodies revealed that most autoepitopes are in different sites in GPIb $\alpha$ .<sup>25</sup> In addition, anti-GPIb $\alpha$  antibodies can induce profound irreversible thrombocytopenia by an Fc-independent mechanism.<sup>26</sup> As the intermembrane distance of the immunologic synapse is a critical design parameter of the ligand-binding domain,<sup>27</sup> various truncated forms of GPIb $\alpha$  were used as the targeting domain in the study.

In this work, we proposed a new strategy for immunotherapy for ITP in which autoantigen-modified T cells function like a Trojan horse to trap autoreactive B cells and perform specific killing. We constructed the GPIb $\alpha$  fragment into the second-generation CAR structure and verified that GPIb $\alpha$  CAAR T cells function as expected *in vitro* and *in vivo*. GPIb $\alpha$  CAAR T is a precision cellular immunotherapy with potential to induce complete and durable remission of refractory and relapsed ITP patients.

## Methods

Animal experiments were approved by the Ethics Committee of Tongji Medical College, Huazhong University of Science and Technology (IACUC no. 3284). Experiments involving humans were conducted per the Declaration of Helsinki and were approved by the Ethics Committee of Union Hospital, Tongji Medical College, Huazhong University of Science and Technology (IEC-J (487)).

### GPIb $\alpha$ chimeric autoantibody receptor plasmid construction

The native GPIb $\alpha$  ectodomain of various lengths was constructed into a second-generation CAR structure containing a CD8 $\alpha$  hinge/transmembrane region, 4-1BB co-stimulatory domain, and intracellular CD3 $\zeta$  domain. Lentiviral vectors with or without green fluorescent protein (GFP) expression were used. GFP was linked with the CAAR fragment to facilitate the detection of GPIb $\alpha$  CAAR expression. The GPIb $\alpha$  mutant plasmid was constructed using the QuikChange Site-Directed Mutagenesis Kit.

### Modified light transmission analysis

CAAR3 and GPIb $\alpha$  residue 233-mutated CAAR3 (CAAR3-mut-g233k) were expressed on the Jurkat T-cell surface with lentivirus transduction. Jurkat-CAAR3-T and Jurkat-CAAR3-mut-g233k T cells were resuspended to a concentration of 10<sup>7</sup> cells/mL, and 300  $\mu$ L of cell suspension was added to a colorimetric cup. Then, 5  $\mu$ g/mL human VWF was added in the presence of 0.25 mg/mL ristocetin. Under the shear force and the induction of ristocetin,<sup>16</sup> the VWF protein binds to Jurkat T cells expressing extracellular domains of GPIb $\alpha$  (CAAR3) on the surface, eventually triggering an aggregation reaction of the cells, which can be measured as an increase in light transmission collected by a platelet aggregation analyzer.

### *In vitro* cytotoxicity assays

Donor-matched non-transduced T (NTD-T) cells or GPIb $\alpha$  CAAR T cells were co-incubated with control hybridoma (PE) and the target anti-GPIb $\alpha$  hybridoma cells (APC) at an effector to target (E:T) ratio of 5:1, while the ratio of target hybridoma cells to control hybridoma cells was 3:1. Cytotoxicity was evaluated at 24 hours using flow cytometry based on the changes in the ratio of target hybridoma cells to control hybridoma cells.

### Anti-GPIb $\alpha$ hybridoma xenograft models

Six-to-eight-week-old NSG mice (NOD-scid IL2R $\gamma$ null) were intravenously inoculated with anti-GPIb $\alpha$  B cells (10<sup>5</sup> cells per mouse), followed 2 days later by injection with LBD-mutg233k T cells or NTD T cells (10<sup>7</sup> cells per mouse), and monitored for engraftment and therapeutic response by the IVIS<sup>®</sup> system every few days.

### Cytometric bead array

The microbeads carrying different fluorescence (APC) intensities were separately coated with monoclonal antibodies: anti-GPIX (clone: sz-1), anti-granule membrane protein (GMP) 140 (clone: sz-51), anti-GPIb (clone: sz-2), anti-GPIIb (clone: sz-22), and anti-GPIIIa (clone: sz-21). Platelets were isolated from ITP patients or healthy controls, then platelet lysate was incubated with the coated microbeads, followed by FITC-conjugated goat-anti-human IgG polyclonal antibodies, and finally analyzed with flow cytometry.

### GPIb $\alpha$ enzyme-linked immunospot assay

GPIb $\alpha$  CAAR T-cell-specific cytolysis of anti-GPIb $\alpha$  antibody-producing human B cells was measured using an enzyme-linked immunospot (ELISpot) assay. peripheral blood mononuclear cells isolated from patients and healthy control were stimulated and then incubated with GPIb $\alpha$  CAAR T cells, anti-CD19 CAR T cells, or NTD T cells on the polyvinylidene difluoride-bottomed microplate coated with human GPIb $\alpha$  protein, anti-human IgG antibody, or BSA. Specific antibodies secreted by B cells will form spots on the microplates, which can be counted.

Details on these protocols and additional methods are provided in the *Online Supplementary Appendix*.

## Results

### Development of GPIb $\alpha$ chimeric autoantibody receptor plasmids

GPIb $\alpha$  is the largest subunit of the GPIb-IX complex (Figure 1A), and 282 N-terminal membrane-distal residues, which are composed of seven leucine-rich repeats (LRR), make up the ligand-binding domain (LBD), which binds to VWF and other ligands. The VWF binding region is followed by a heavily O-glycosylated macroglycopeptide domain and a mechanosensory domain (MSD).<sup>28</sup> Anti-LBD antibodies are

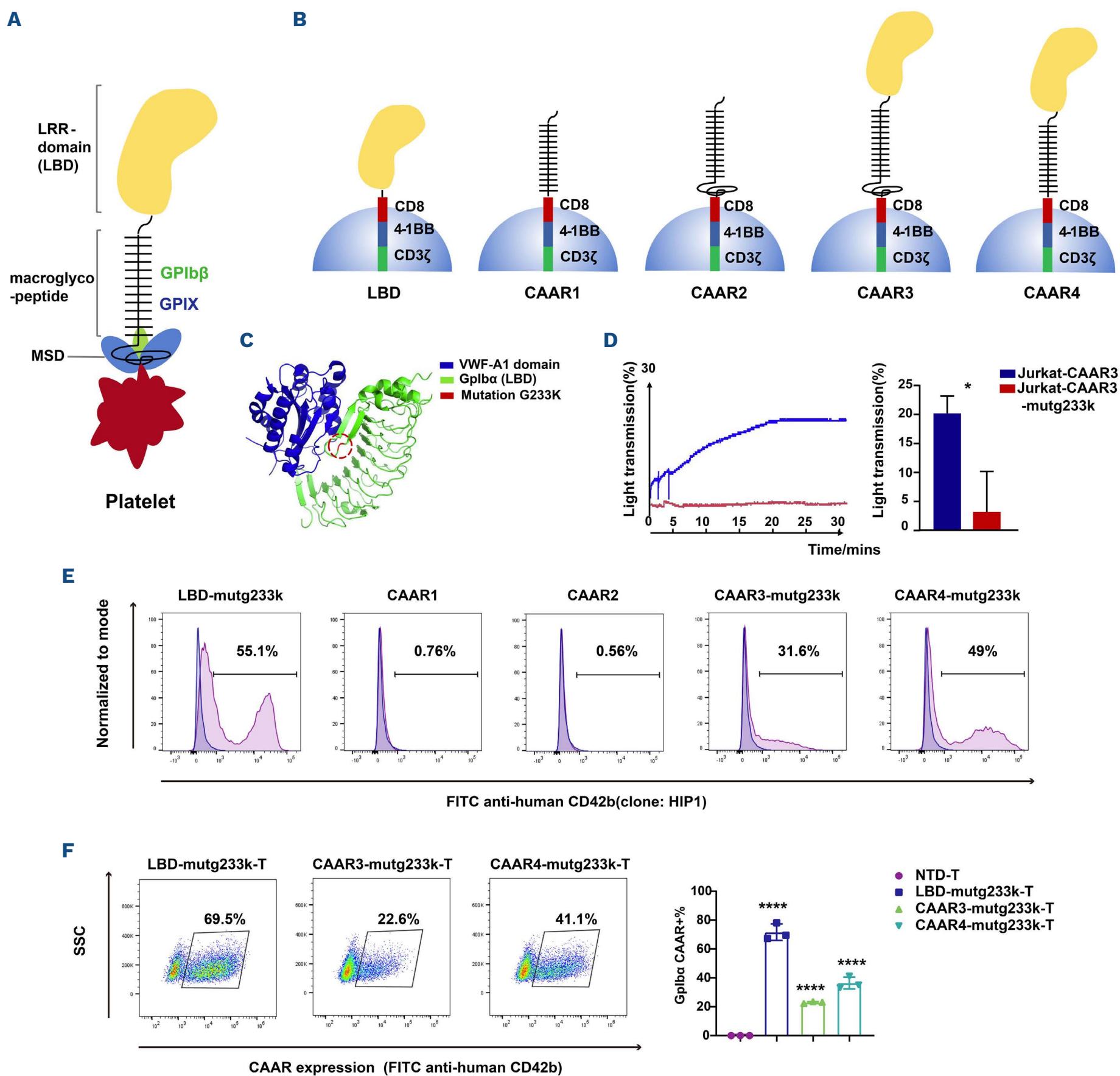


**Figure 1. Construction and validation of the GPIIb $\alpha$  chimeric autoantibody receptor structure.** (A) The GPIIb-IX complex contains GPIIb $\alpha$ , GPIIb $\beta$  (green), and GPIIX (blue); GPIIb $\alpha$  is the largest subunit. GPIIb $\alpha$  is composed of seven leucine-rich repeats (LRR), make up the ligand-binding domain (LBD), followed by a heavily O-glycosylated macroglycopeptide domain and a mechanosensory domain (MSD). (B) Schematic of GPIIb $\alpha$  chimeric autoantibody receptor (CAAR) constructs comprising diverse lengths of the native GPIIb $\alpha$  ectodomain, followed by the CD8 $\alpha$  transmembrane domain and 4-1BB-CD3 $\zeta$  intracellular co-stimulatory and activation domains, named LBD, CAAR1, CAAR2, CAAR3, and CAAR4. (C) Crystal structures (Protein data bank ID: 1m10) of the NH<sub>2</sub>-terminal domain of GPIIb $\alpha$  (green, residues 1 to 290) and its complex with the von Willebrand Factor (VWF) A1 domain (blue, residues 498 to 705) are shown, and the loss-of-function mutation at residue 233 of GPIIb $\alpha$  (red, G233K) is indicated. (D) Ristocetin-induced VWF binding to GPIIb $\alpha$  fragments expressed on Jurkat T cells. CAAR3 and residue 233-mutated CAAR3 (CAAR3-mutg233k) were expressed on the surface of Jurkat T cells, and cell aggregation was measured as an increase in light transmission (%) (N=3; \**P*<0.05). (E) In order to identify the mature conformational epitopes, mutated-GPIIb $\alpha$  CAAR plasmids were transfected into HEK293T cells, and then the cells were stained with an anti-human CD42b (GPIIb $\alpha$ ) antibody (clone: HIP1). (F) At a multiplicity of infection (MOI) of 25, primary human T cells were transduced with LBD-mutg233k-CAAR, CAAR3-mutg233k-CAAR, and CAAR4-mutg233k-CAAR lentivirus, and CAAR expression was determined using an anti-human CD42b antibody (clone: HIP1). The transduction efficiency of GPIIb $\alpha$  CAAR<sup>+</sup> in T cells from 3 healthy donors was calculated. SSC: side scatter; NTD T: non-transduced T cells. \*\*\*\**P*<0.0001.

associated with refractoriness to IVIg or steroids in ITP patients,<sup>23,26,29</sup> and the MSD juxtamembrane portion of GPIIb $\alpha$  is related to ligand binding and signal transduction.<sup>30</sup> Native GPIIb $\alpha$  ectodomains of various lengths (LBD/CAAR1/CAAR2/CAAR3/CAAR4) were constructed into a second-generation CAR structure containing a CD8 $\alpha$  hinge/transmembrane region, 4-1BB co-stimulatory domain, and intracellular CD3 $\zeta$  domain, as shown in Figure 1B and *Online Supplementary Figure S1*. LBD CAAR contains the LRR domain; CAAR1 contains the macroglycopeptide domain; CAAR2 contains the macroglycopeptide domain plus MSD; CAAR3 comprises the LRR domain, the macroglycopeptide domain, and MSD; and CAAR4 consists of the LRR domain and the macroglycopeptide domain. The five CAAR structures were first expressed on the surface of HEK293T cells, and the proper conformation of the CAAR structures was verified by the anti-human platelet GPIIb $\alpha$  antibody (clone: HIP1). As shown in *Online Supplementary Figure S2A*, CAAR expression was successfully detected in LBD CAAR, CAAR3, and CAAR4 but not in CAAR structures that did not contain LBD (CAAR1, CAAR2), probably because this antibody recognizes a site in the LBD. The above results preliminarily proved that the conformational epitope of GPIIb $\alpha$  CAARs is consistent with that of native human platelet GPIIb $\alpha$ . CAAR expression in primary human T cells was also detected. T cells were transduced with GPIIb $\alpha$ -CAAR lentivirus (multiplicity of infection 25 to 100), and the transduction efficiencies of GPIIb $\alpha$  CAAR T cells were determined with an anti-human platelet GPIIb $\alpha$  antibody (clone: HIP1) by flow cytometry (*Online Supplementary Figure S2B*).

### **GPIIb $\alpha$ G233K mutation inhibited von Willebrand factor binding to GPIIb $\alpha$ chimeric autoantibody receptor T cells**

The platelet surface membrane protein GPIIb $\alpha$  participates in platelet plug formation by binding to the A1 domain of VWF, which is already attached to the subendothelium.<sup>16</sup> The  $\beta$ -switch region (AAs 227-241) of GPIIb $\alpha$  plays an essential role in forming the GPIIb $\alpha$ -VWF complex, and residue 233 plays a critical role in regulating VWF binding.<sup>31-33</sup> The crystal structures of the NH<sub>2</sub>-terminal domain of GPIIb $\alpha$  (residues 1 to 290) and its complex with the VWF-A1 domain (residues 498 to 705) are shown in Figure 1C. In order to avoid affecting the regular role of the GPIIb $\alpha$ -VWF complex in the process of hemostasis after CAAR T-cell infusion, we chose residue 233 (G233K) of GPIIb $\alpha$  for mutation in the CAAR structure. CAAR3 and GPIIb $\alpha$  residue 233-mutated CAAR3 (CAAR3-mutg233k) were expressed on the Jurkat T-cell surface with lentivirus transduction. As shown in the aggregometry measurements in Figure 1D, under shear force and induction by ristocetin, the VWF protein bound to Jurkat-CAAR3 T cells, triggering a cell aggregation reaction, and an increase in light transmission was observed, which was not detected in the Jurkat-CAAR3-mutg233k T-cell group. The results demonstrated that the G233K mutation of GPIIb $\alpha$  expressed on the cell surface strongly

inhibits its binding to VWF, which could alleviate possible off-target effects after CAAR T-cell infusion *in vivo*. The mutated GPIIb $\alpha$  CAAR structures were named LBD-mutg233k, CAAR3-mutg233k, and CAAR4-mutg233k, and the integrity of the CAAR epitopes was confirmed with HIP1 (Figure 1E). The transduction efficiencies of the mutated GPIIb $\alpha$  CAAR T cells are presented in Figure 1F. At a multiplicity of infection (MOI) of 25, LBD-mutg233k T cells exhibited the highest transduction efficiency, followed by CAAR4-mutg233k T and CAAR3-mutg233k T cells. The size of the CAAR fragment was an essential factor affecting the transfection efficiency as indicated, and the results from three healthy donor T cells are shown (Figure 1F).

### **Generation of four anti-GPIIb $\alpha$ hybridomas with different chimeric autoantibody receptor binding sites**

In order to generate hybridomas and antibodies that bind to human platelet GPIIb $\alpha$ , washed human platelet lysate was used as the antigen for mouse immunization, and mouse serum was screened by GPIIb $\alpha$  enzyme-linked immunosorbent assay (ELISA). The four selected anti-GPIIb $\alpha$  hybridomas were named Gvb1, Gvb2, Gvb3, and Gvb4. Human platelets were incubated with each APC-conjugated hybridoma antibody (Gvb1/Gvb2/Gvb3/Gvb4) and FITC-anti-human CD42b antibody simultaneously to analyze the ability of the acquired antibodies to bind to human platelets. The flow cytometry results (Figure 2A) showed that the four anti-GPIIb $\alpha$  antibodies could bind to human platelets, demonstrating their ability to bind with the native conformation epitope of GPIIb $\alpha$ . As target cell surface antigen density might affect CAR T-cell cytolytic efficiency,<sup>27</sup> the density of BCR on the surface of each hybridoma was then measured with an anti-mouse IgG antibody (APC-conjugated). The BCR mean fluorescence intensity (MFI) of the four hybridomas is presented in Figure 2B, varying among the anti-GPIIb $\alpha$  hybridomas, and the Gvb3 hybridoma showed the highest surface BCR density, followed by the Gvb1, Gvb2, and Gvb4 hybridomas.

In order to verify the binding ability of the hybridoma antibodies to mutated GPIIb $\alpha$  CAAR and identify the binding sites between them, we further expressed mutated GPIIb $\alpha$  CAAR in HEK293T cells. The proportion of cells that bound to the hybridoma antibodies in total GPIIb $\alpha$  CAAR-GFP-expressing cells (Q2/(Q2+Q3)) was determined and represented the binding force between the hybridoma antibodies and CAAR. As shown in Figure 2C-F, Gvb1, Gvb2, and Gvb3 could bind to LBD-mutg233k-CAAR, CAAR3-mutg233k-CAAR, and CAAR4-mutg233k-CAAR, while Gvb4 could bind to all GPIIb $\alpha$  CAAR. The locus recognized by Gvb4 is thus in the overlapping part of LBD-mutg233k-CAAR and CAAR1/CAAR2. The findings revealed that though the binding epitopes of each hybridoma antibody to the CAAR should be similar, the binding efficiencies varied. Gvb4 could bind to all GPIIb $\alpha$  CAAR, proving that its binding site is the same site shared by the above CAAR but exhibited different binding effi-

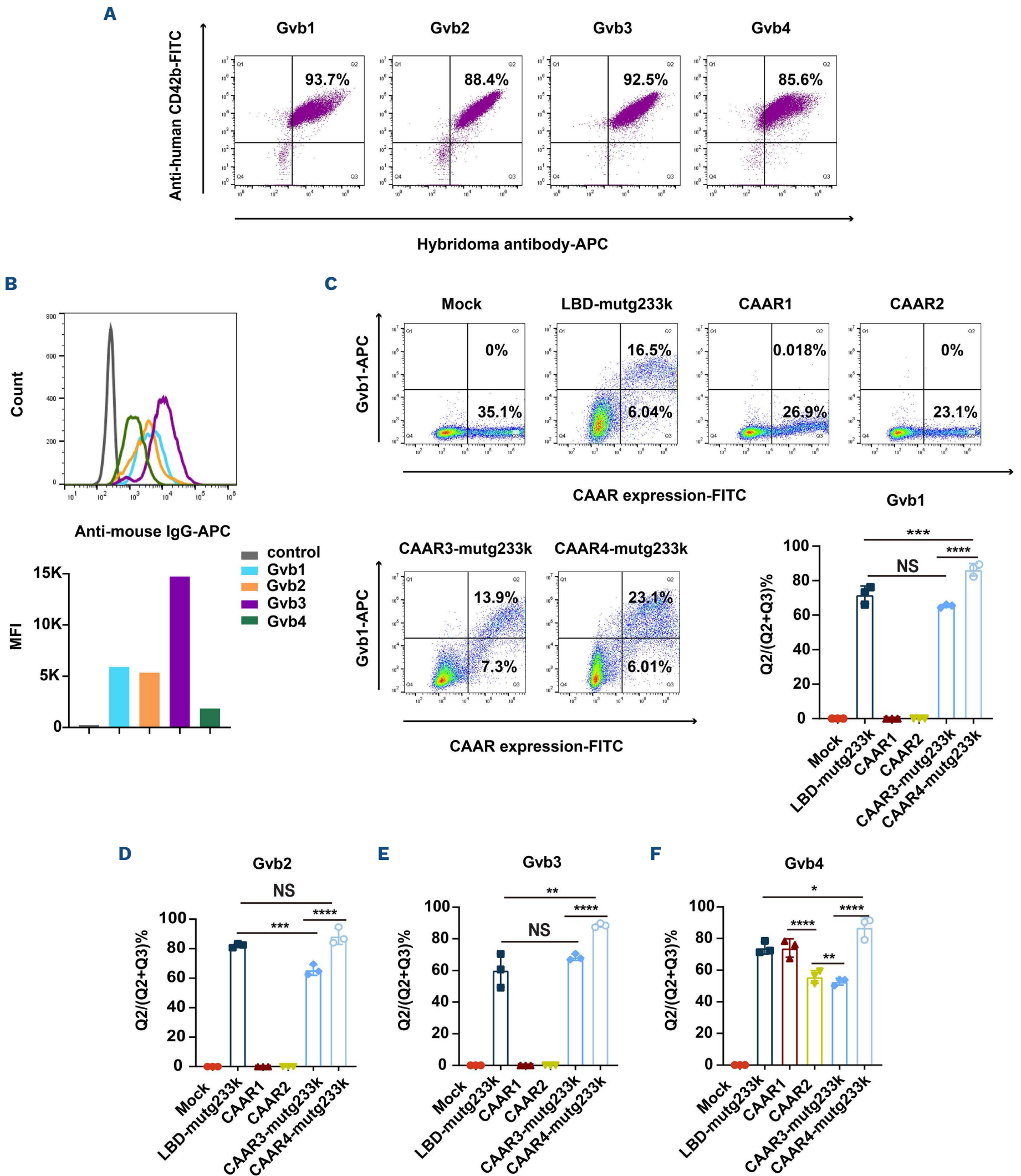


**Figure 2. Generation of four anti-GPIIb $\alpha$  hybridoma antibodies and validation of their binding epitopes with GPIIb $\alpha$  chimeric autoantibody receptors.** (A) Binding detection of the 4 anti-GPIIb $\alpha$  hybridoma antibodies (Gvb1/Gvb2/Gvb3/Gvb4) to human platelets using flow cytometry. Platelets were incubated with anti-human CD42b (GPIIb $\alpha$ ) antibody (clone: HIP1) and each anti-GPIIb $\alpha$  hybridoma antibody (APC-conjugated) simultaneously. (B) B-cell receptor (BCR) density quantification for the 4 anti-GPIIb $\alpha$  hybridoma cells. Hybridoma cells were stained with goat anti-mouse IgG antibodies (APC-conjugated). The mean fluorescence intensity (MFI) of BCR expression is shown in a histogram and bar graph. (C-F) Identification of the different binding epitopes of the hybridoma antibodies Gvb1, Gvb2, Gvb3, and Gvb4. Mock, LBD-mutg233k, CAAR1, CAAR2, CAAR3-mutg233k, CAAR4-mutg233k. NS, not significant; \*\* p < 0.01; \*\*\* p < 0.001; \*\*\*\* p < 0.0001.

Continued on following page.

Gvb4 to mutated GPIb $\alpha$  chimeric autoantibody receptor (CAAR) structures. GPIb $\alpha$  CAAR were expressed on the surface of HEK293T cells, which were incubated with each hybridoma antibody (APC-conjugated). Green fluorescent protein (GFP) was linked with the CAAR fragment to facilitate the detection of GPIb $\alpha$  CAAR expression. The binding force between each hybridoma antibody and the CAAR was calculated as the ratio of cells bound to hybridoma antibodies in total GPIb $\alpha$  CAAR-GFP-expressing cells ( $Q_2/(Q_2+Q_3)$ ). NS: not significant  $P>0.05$ ; \* $P<0.05$ ; \*\* $P<0.01$ ; \*\*\* $P<0.005$ ; \*\*\*\* $P<0.0001$ .

ciencies to these CAAR; this suggested that the different CAAR structures had different spatial conformations that may affect the binding force of the hybridoma antibody. In summary, we obtained four hybridomas with different binding sites that could simulate B cells from ITP patients with different anti-GPIb $\alpha$  epitopes for further CAAR T-cell cytolytic assays. As Gvb4 could bind to all the CAAR (Figure 2F), the transduction efficiencies of GPIb $\alpha$  CAAR T cells were determined using the APC-conjugated hybridoma antibody Gvb4, as shown in *Online Supplementary Figure S2C*.

### **In vitro, GPIb $\alpha$ chimeric autoantibody receptor T cells exhibited specific cytotoxicity of autoreactive B cells**

In order to verify the specific lysis of autoreactive B cells by GPIb $\alpha$  CAAR T cells, NTD T or GPIb $\alpha$  CAAR T cells were incubated with each anti-GPIb $\alpha$  hybridoma various at ratios ranging from 1:1 to 10:1. At 16 hours postincubation, the medium supernatants were collected and measured immediately for LDH activity. GPIb $\alpha$  CAAR T cells demonstrated specific lysis of autoreactive B cells (Gvb1/Gvb2/Gvb3/Gvb4) targeting different GPIb $\alpha$  domains in a manner dependent on the E:T ratio and NTD T cells showed no cytotoxicity (Figure 3A). Notably, the pernicious effects of GPIb $\alpha$  CAAR T cells varied due to variations in binding epitopes of the target cell to CAAR, and LBD-mutg233k T cells exhibited the most robust cytotoxicity function against the four hybridomas. We also performed cytotoxicity assays with flow cytometry to further prove the specific cytolytic function of the CAAR T cells. NTD T or LBD-mutg233k T cells were coincubated with hybridoma control and the target anti-GPIb $\alpha$  hybridoma cells. The original ratio of target hybridoma cells to control hybridoma cells was 3:1. As shown in Figure 3B-E, due to the specific lysis of target hybridoma cells by LBD-mutg233k T cells, the ratio of target cells to control cells in the co-culture system decreased significantly compared with that in the NTD T group. Similar results for CAAR3-mutg233k T, CAAR4-mutg233k T, CAAR1 T, and CAAR2 T cells were obtained and are presented in *Online Supplementary Figure S3*. High levels of the pro-inflammatory cytokines (Figure 3F) IL-2 and interferon (IFN)- $\gamma$  were secreted by T cells after stimulation with each target hybridoma and varied among different GPIb $\alpha$  CAAR T cells and tested extremely low in the NTD T groups. Consistent with the binding assay results (Figure 2C-F), even though the binding sites of GPIb $\alpha$  CAAR and each hybridoma were similar, the difference brought about by the spatial conformation of the CAAR eventually resulted in differences in the binding forces and cytolytic functions of the GPIb $\alpha$  CAAR T cells. LBD-mutg233k T cells showed

a stable spatial conformation and robust cytolytic ability. CAAR4-mutg233k T cells, comprising the LBD and a heavily O-glycosylated macroglycopeptide domain, exhibited the most potent binding with hybridoma antibodies, and the cytolytic efficiency was inferior to that of LBD-mutg233k T cells. CAAR3-mutg233k-CAAR has an extra MSD structure and a poorer killing effect than CAAR4-mutg233k-CAAR. The MSD structure's instability<sup>28</sup> may influence the binding of CAAR3-mutg233k T cells and anti-GPIb $\alpha$  hybridomas, possibly accounting for the lower killing efficiency.

### **Soluble anti-GPIb $\alpha$ antibodies slightly affect GPIb $\alpha$ chimeric autoantibody receptor T-cell cytotoxicity**

Soluble autoantibodies can either prevent CAAR contact with anti-CAAR BCR or enhance cytotoxicity by activating CAAR T cells; therefore, their impact on CAAR T-cell cytotoxicity is erratic.<sup>14,15</sup> In order to determine soluble anti-GPIb $\alpha$  antibody effects on GPIb $\alpha$  CAAR T-cell activity, we performed cytotoxicity assays in the presence of a wide range of concentrations (0-40  $\mu\text{g}/\text{mL}$ ) of monoclonal antibodies (mAb) or mixed mAb, as no quantitative data on plasma anti-GPIb $\alpha$  IgG concentration in ITP patients were currently available. GPIb $\alpha$  CAAR T-cell cytotoxicity against hybrid target cells (Gvb1/Gvb2/Gvb3/Gvb4) was mildly increased with higher effector-to-target ratios in the presence of soluble anti-GPIb $\alpha$  polyclonal IgG (a mixture of Gvb1, Gvb2, Gvb3, and Gvb4, and the concentration of each antibody is 5  $\mu\text{g}/\text{mL}$ ) (Figure 4A), as were IFN- $\gamma$  levels (Figure 4B). Then, NTD T or LBD-mutg233k T cells and mixed target cells were incubated with each anti-GPIb $\alpha$  mAb at various concentrations (0, 10, 20, or 40  $\mu\text{g}/\text{mL}$ ). Cytotoxicity (Figure 4C) and IFN- $\gamma$  levels (Figure 4D) were slightly affected in a concentration-related manner and varied among the anti-GPIb $\alpha$  mAb. The cytolytic efficiency of CAAR T cells and the IFN- $\gamma$  levels were marginally enhanced or somewhat reduced with increasing antibody concentration in different groups. Therefore, we conclude that the impact of soluble anti-GPIb $\alpha$  mAb on CAAR T-cell function generally varies and is minimal.

### **GPIb $\alpha$ chimeric autoantibody receptor T cells demonstrated in vivo persistence and specific cytolytic activity with no apparent organ toxicity**

A xenograft model was developed to assess the cytolytic efficiency and safety of GPIb $\alpha$  CAAR T cells *in vivo*. Luciferase (Luc)/GFP-expressing anti-GPIb $\alpha$  hybridoma cells ( $10^5$  cells per mouse) and LBD-mutg233k T cells ( $10^7$  cells per mouse) were intravenously injected into 6-8-week-old NSG mice, which were examined for engraftment and therapeutic re-

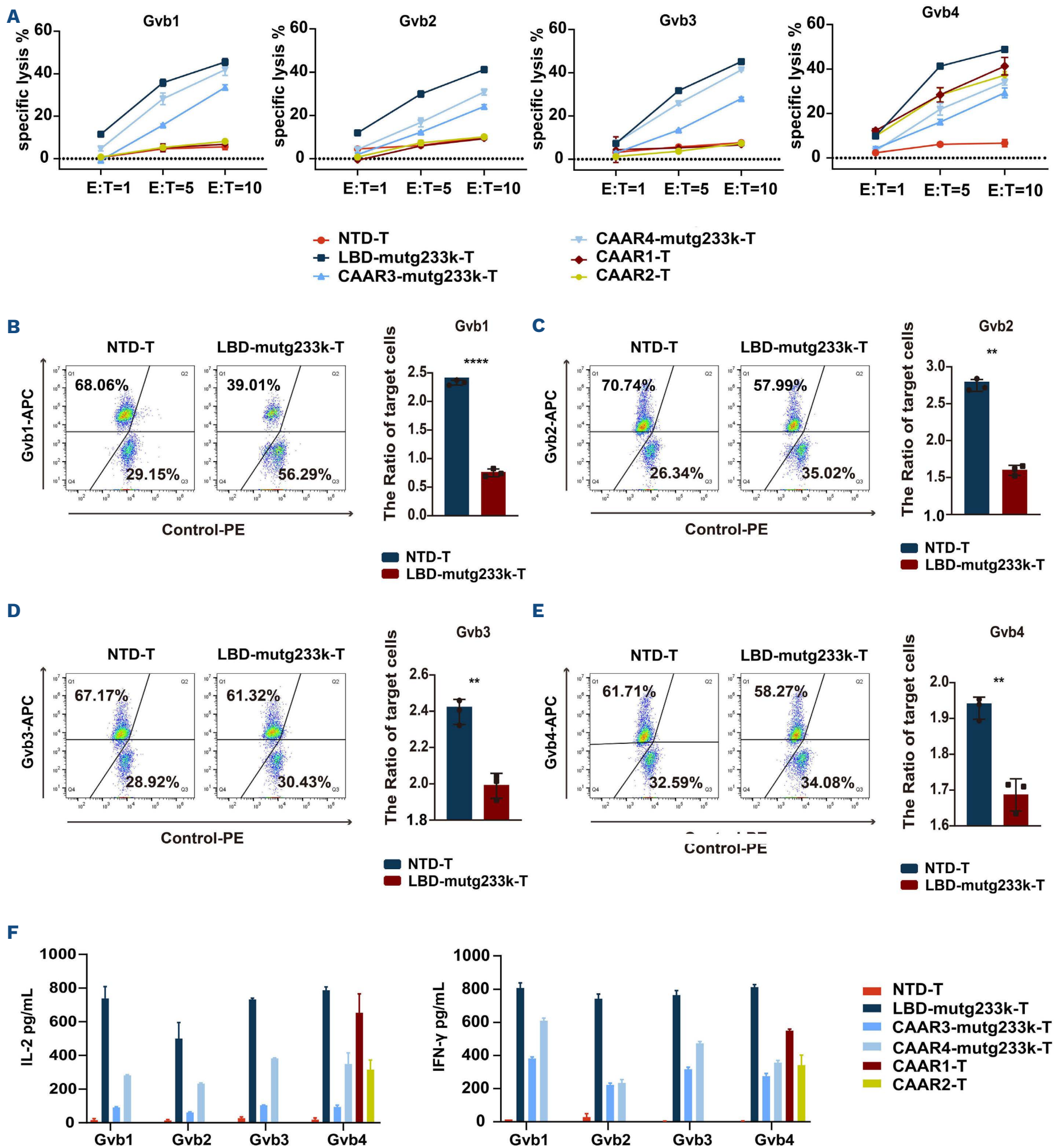
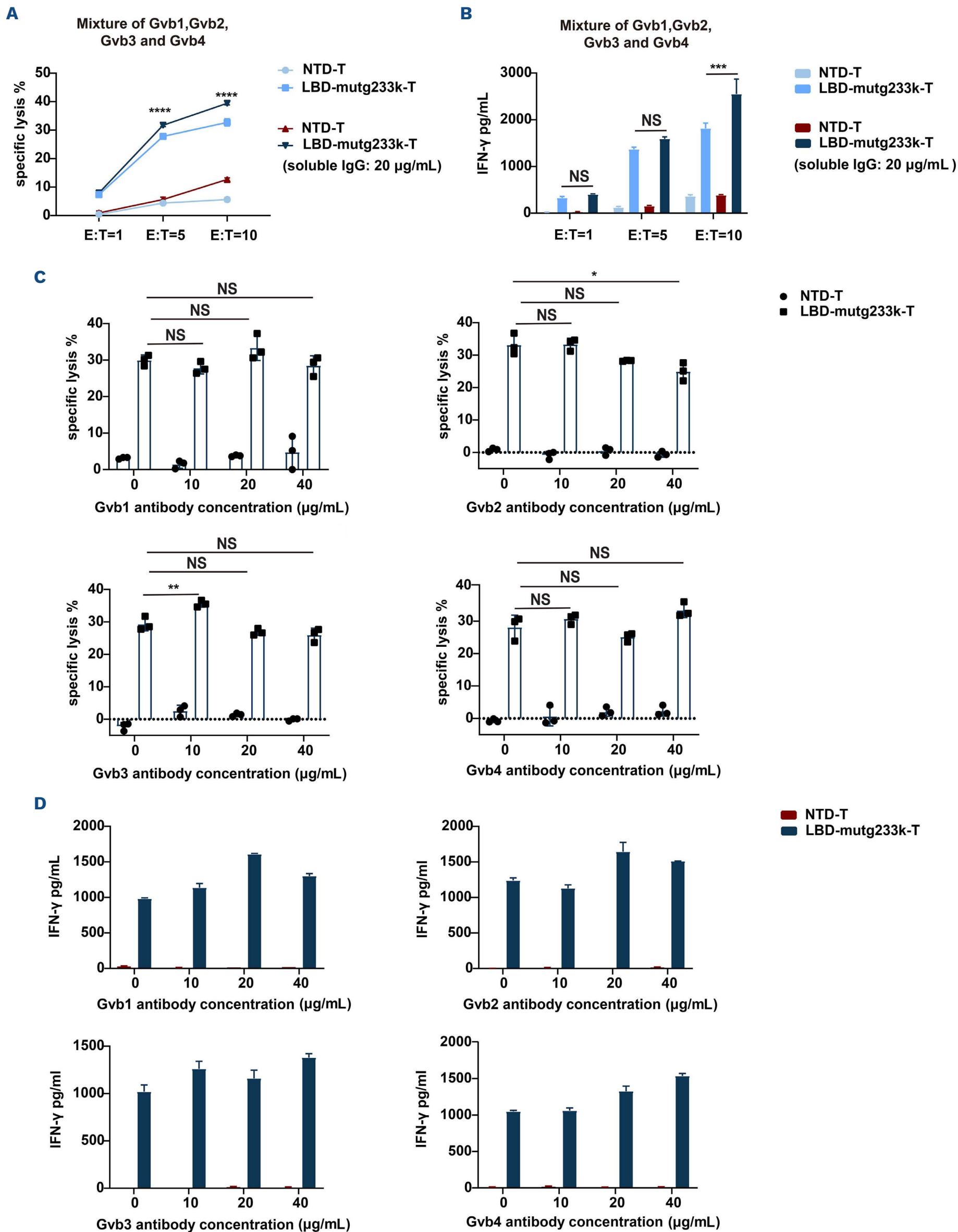


**Figure 3. GPIb $\alpha$  chimeric autoantibody receptor expression on primary human T cells directs specific cytotoxicity of anti-GPIb $\alpha$  B cells *in vitro*.** (A) Hybridoma cells (Gvb1/Gvb2/Gvb3/Gvb4) were co-incubated with non-transduced T cells (NTD T) or GPIb $\alpha$  chimeric autoantibody receptor (CAAR) T cells at the indicated effector to target (E:T) ratios for 16 hours. Specific lysis was measured by lactate dehydrogenase (LDH) release into the supernatant. (B-E) NTD T or LBD-mutg233k T cells were co-incubated with control hybridoma (PE) and anti-GPIb $\alpha$  hybridomas (APC) at an E:T ratio of 5:1. The ratio of the target hybridoma to total control hybridoma cells was 3:1. Cytotoxicity was evaluated at 24 hours using flow cytometry, as indicated by the changes in the ratio of the target hybridoma to the control hybridoma. \*\* $P < 0.01$ ; \*\*\*\* $P < 0.0001$ . (F) Cytokines (interleukin [IL]-2, interferon [IFN]- $\gamma$ ) produced by NTD T or GPIb $\alpha$  CAAR T cells after 5:1 co-culture with each anti-GPIb $\alpha$  hybridoma cell for 16 hours, as measured in the supernatant by enzyme-linked immunosorbant assay.



Continued on following page.

**Figure 4. Evaluation of soluble anti-GPIb $\alpha$  antibody effects on GPIb $\alpha$  chimeric autoantibody receptor T-cell cytotoxicity.** (A) Non-transduced T cells (NTD T) or LBD-mut223k T cells were co-incubated with a mixture of the 4 anti-GPIb $\alpha$  target cells at the indicated effector to target (E:T) ratios in the presence or absence of soluble anti-GPIb $\alpha$  immunoglobulin (Ig)G polyclonal antibody (a mixture of Gvb1, Gvb2, Gvb3, and Gvb4, and the concentration of each antibody is 5  $\mu$ g/mL). Cytotoxicity was evaluated at 16 hours by lactate dehydrogenase (LDH) release assay. Meanwhile, human interferon (IFN)- $\gamma$  (B) in cell culture supernatants was quantitated by enzyme-linked immunosorbent assay (ELISA) after 16 hours. (C-D) NTD T or LBD-mutg233k T cells were incubated with each anti-GPIb $\alpha$  IgG monoclonal antibody (0, 10, 20, or 40  $\mu$ g/mL) at an E:T ratio of 5. Cytotoxicity was evaluated at 16 hours by LDH release assay, and human IFN- $\gamma$  in cell culture supernatants was quantitated by ELISA after 16 hours. NS: not significant  $P>0.05$ ; \* $P<0.05$ ; \*\* $P<0.01$ ; \*\*\* $P<0.005$ ; \*\*\*\* $P<0.0001$ .

response. Mice treated with NTD T cells were used to monitor the allogenic effects. Bioluminescence imaging indicated that GPIb $\alpha$  CAAR T cells significantly reduced anti-GPIb $\alpha$  hybridoma outgrowth compared to NTD T cells (Figure 5A). From the 14<sup>th</sup> day to the 21<sup>st</sup> day, the autoreactive B-cell burden (mean ROI) of the LBD-mutg233k T-treated mice 3 and 4 (T3 and T4) decreased from 4,096.406 to 1,028.801 and 28,029.28 to 2,671.87 (photons/s/cm<sup>2</sup>/sr), respectively (Figure 5B). Total human T cells and CAAR T cells in peripheral blood (PB) were monitored every few days (Figure 5C). PB T cells of the CAAR T-treated mice proliferated rapidly from day 18 to day 24, far exceeding the proliferation of the NTD T group, which encounters with target cells can explain. Control and LBD-mutg233k T-cell-treated mice were euthanized 21–28 days after hybridoma cell/T-cell injection, and T-cell persistence and penetration in bone marrow, spleen, and blood samples were assessed by flow cytometry. Consistent with the PB results, T cells of the CAAR T-treated mice isolated from the spleen and bone marrow exhibited a more potent ability to persist and proliferate *in vivo* than T cells in the control group, as shown in Figure 5D, E. Immunofluorescence imaging (*Online Supplementary Figure S4A*) also indicated lymphocyte infiltration and persistence in the liver and spleen. The plasma anti-GPIb $\alpha$  antibody titer increased in mice treated with NTD T cells from day 7 to 21. In contrast, the titers in GPIb $\alpha$  CAAR T-cell-treated mice were significantly reduced compared to those in NTD T-cell-treated mice by day 21 after T-cell injection (Figure 5F). The reduced serum anti-GPIb $\alpha$  ELISA results also reflected hybridoma control in LBD-mutg233k T-treated mice. Off-target cytotoxic effects of GPIb $\alpha$ -CAAR T cells on mice were not observed, as hematoxylin and eosin (H&E) staining revealed that the morphology of tissues and organs in mice did not change significantly, and serum biochemical levels were normal (*Online Supplementary Figure S4B, C*). In conclusion, GPIb $\alpha$  CAAR T cells demonstrated *in vivo* persistence and specific cytolytic capacity with no apparent organ toxicity.

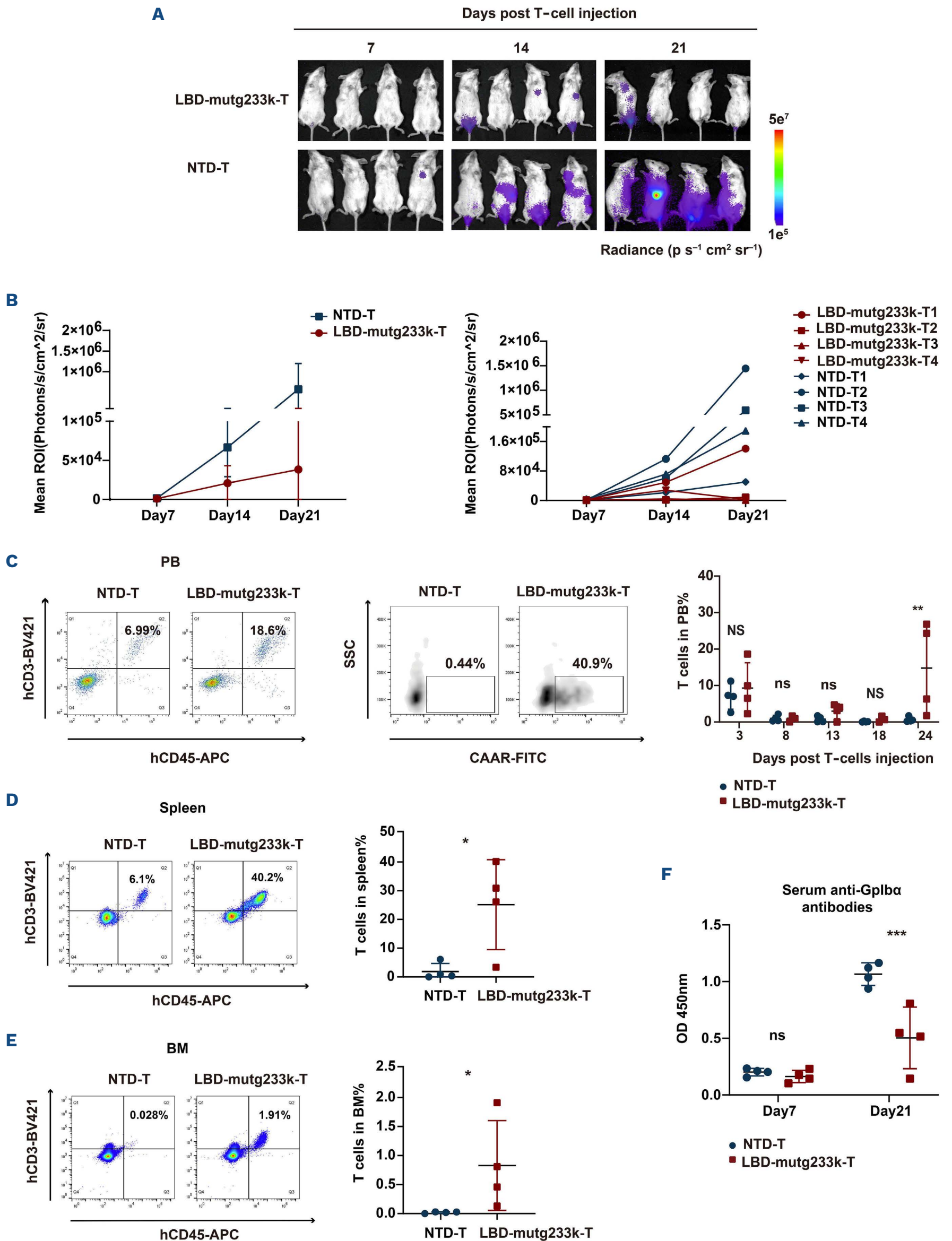
#### **GPIb $\alpha$ chimeric autoantibody receptor T cells showed potential in eradicating autoreactive B cells of immune thrombocytopenia patients**

In order to test the ability of GPIb $\alpha$  CAAR T cells to interact with native GPIb $\alpha$  autoantibodies from ITP patients, a plasma antibody binding assay (Figure 6A; *Online Supplementary Figure S5A*) was first applied. Patients diagnosed

with primary ITP were included and tested for specific platelet autoantibodies using a cytometric bead array (Figure 6B; *Online Supplementary Figure S5B*). Sera from three ITP patients with anti-GPIb antibodies and healthy controls were diluted at 1:10 and 1:20 and then incubated with HEK293T cells expressing the LBD-mutg233k-CAAR structure tagged with GFP. After incubation, the cells were stained with APC-anti-human immunoglobulin (Ig)G antibodies. The flow cytometry results (Figure 6A) showed that the serum anti-GPIb $\alpha$  antibodies of patient 3 could react with LBD-mutg233k-CAAR, but no binding of patient 1 and patient 2 plasma antibodies to LBD-mutg233k-CAAR was detected. A possible explanation for this negative result is that platelet lysates were used to screen patients with anti-GPIb antibodies, and the level of platelet antibodies in the lysates is much higher than the platelet antibodies in the plasma. At the same time, we examined the binding reaction of plasma from patient 3 to CAAR3-mutg233k-CAAR and CAAR4-mutg233k-CAAR. Interestingly, although CAAR3-mutg233k-CAAR and CAAR4-mutg233k-CAAR contained fragments of LBD-mutg233k-CAAR, they did not react with serum antibodies from patient 3, and the results are presented in *Online Supplementary Figure S5A*. The ELISpot assay was employed to verify GPIb $\alpha$  CAAR T-cell potential in eradicating autoreactive B cells in ITP patients. ELISpot analysis (Figure 6C) showed that anti-GPIb $\alpha$  IgG B cells, but not total IgG B cells from ITP patients, were depleted by GPIb $\alpha$  CAAR T cells. Meanwhile, anti-CD19 CAR T cells eliminated all IgG B cells from ITP patients and healthy controls. In summary, we confirmed the viability of the “Trojan hypothesis” for the treatment of ITP patients. GPIb $\alpha$  CAAR T cells function like a “Trojan horse”, trapping autoreactive B cells and performing specific killing. (Figure 6D)

## **Discussion**

Our study presents a novel concept for the treatment of refractory and relapsed ITP patients with autoantigen-modified T cells based on CAR T cells. Since patients with anti-GPIb $\alpha$  antibodies have a poor response to standard immunosuppressive therapy, GPIb $\alpha$  was constructed into the ligand-binding domain of the CAAR structure in this study. Anti-GPIb $\alpha$  antibodies can cause platelet desialylation, mediate Fc-independent platelet eradication,<sup>34,35</sup> affect thrombopoietin production in the liver, and account for



Continued on following page.

**Figure 5. GPIb $\alpha$  chimeric autoantibody receptor T cells mediated autoreactive B-cell depletion *in vivo*.** (A) Anti-GPIb $\alpha$  B cells and ligand-binding domain LBD-mutg233k T cells were intravenously inoculated into 7-week-old female NSG mice. Autoreactive B-cell burden was monitored via bioluminescence imaging every few days. (B) Quantification of the autoreactive B-cell burden indicated by the radiance detected in the region of interest with group values or individual values. T1, 2, 3, 4 mean mice 1, 2, 3, 4. (C) Flow cytometry analysis of total human T cells in the peripheral blood (PB) of non-transduced T cell (NTD T)-treated mice (N=4) and LBD-mutg233k T-treated mice (N=4) monitored every few days. T cells were stained with anti-human CD45 antibody (APC) and anti-human CD3 antibody (BV421). Chimeric autoantibody receptor (CAAR) expression in T cells was detected with an anti-human CD42b antibody (FITC). T-cell penetration and persistence in the spleen (D) and bone marrow (BM) (E) of the mice were analyzed with flow cytometry. T cells were stained with anti-human CD45 antibody (APC) and anti-human CD3 antibody (BV421). (F) The serum anti-GPIb $\alpha$  antibody titer of the mice on day 7 and day 21 was detected by enzyme-linked immunosorbent assay at a dilution ratio of 20. NS: not significant  $P>0.05$ ; \* $P<0.05$ ; \*\* $P<0.01$ ; \*\*\* $P<0.005$ . ROI: region of interest; SSC: side scatter.

the inactivated negative feedback mechanism of megakaryocyte-generated platelets that leads to peripheral platelet destruction.<sup>30,36</sup> In this work, site-mutated GPIb $\alpha$  ectodomain of varying lengths were incorporated into second-generation CAR structures to direct specific T-cell cytotoxicity against autoreactive B cells.

In ITP, no cell immunotherapy targeting B cells is currently used. Compared to CAR T-cell therapy, CAAR T-cell therapy ultimately and precisely removes autoreactive B cells and has fewer side effects due to a lower “tumor” burden.<sup>14</sup> This work demonstrated the *in vitro* cytolytic capacity and persistence of GPIb $\alpha$  CAAR T cells and their ability to eliminate GPIb $\alpha$ -specific B cells *in vivo* precisely. B-cell depletion therapy not only reduces autoantibody production but also reduces splenic CD8<sup>+</sup> T-cell proliferation *in vitro*, as well as the ability of CD8<sup>+</sup> T cells to activate and mediate ITP<sup>37</sup> and T-follicular helper cells in both the spleen and the blood.<sup>38</sup> It is anticipated that B-cell clearance mediated by CAAR T-cell therapy may have an additional impact on moderating immunological dysregulation in ITP patients.

The N-terminus of GPIb $\alpha$  contains binding sites for VWF, and anti-GPIb $\alpha$  antibodies can interfere with normal platelet function by inhibiting GPIb $\alpha$ -VWF-mediated platelet aggregation, which may increase the severity of the patient’s hemorrhage at the same time.<sup>39</sup> In order to prevent the off-target effect caused by the competitive binding of GPIb $\alpha$  CAAR T cells with VWF, we generated mutations (Figure 1B; *Online Supplementary Figure S6*) at residues 231, 232, and 233 of GPIb $\alpha$  (K231V/Q232V/G233k/G233D). The results demonstrated that GPIb $\alpha$  mutations strongly inhibited the binding of GPIb $\alpha$  to VWF, which could alleviate possible off-target effects after CAAR T-cell infusion *in vivo*.

The binding force between CAR T cells and cancer cells and the size of the CAR antigen are related to CAR T-cell efficacy, which may explain the varied cytolytic capacity of the CAAR,<sup>40,41</sup> as shown by the results of the hybridoma antibody binding assay (Figure 2) and *in vitro* cytotoxic assay (Figure 3) in our study. GPIb $\alpha$  CAAR T cells with various truncated forms of GPIb $\alpha$  all exhibited cytotoxicity against anti-GPIb $\alpha$  hybridomas. Meanwhile, the epitopes of autoantibodies are also diverse in ITP patients, so it is feasible to choose the most suitable GPIb $\alpha$  CAAR T-cell

therapy for different patients. The MSD of GPIb $\alpha$  is critical in sensing shear stress and converts this mechanical information into a protein-mediated signal in platelets,<sup>28</sup> the role and structural changes of which were also evaluated in this work. CAAR4-mutg233k-CAAR did not contain the MSD; CAAR4-mutg233k T cells showed a better response to anti-GPIb $\alpha$  autoantibodies and exhibited better killing efficiency than CAAR3-mutg233k T cells, which contain MSD. MSD does affect the spatial conformation of the CAAR and negatively affects subsequent binding and cytolytic functions, which did not seem to be necessary in the CAAR constructs. The same results were also confirmed in cytotoxic assays of CAAR1 and CAAR2 (Figure 3F; *Online Supplementary Figure S3*).

In the *in vivo* study, a hybridoma xenograft model was used, referring to existing research.<sup>14</sup> The four hybridomas were obtained by immunizing BALB/C mice with human platelets. The hybridoma antibodies could only target human GPIb $\alpha$  and could not bind to mouse platelets to mediate platelet destruction in mice; thus, we could not assess whether platelets increase after infusion of CAAR T cells. The humanized mouse model was considered, but previous research<sup>42,43</sup> has shown that human platelets are low in the PB of humanized mouse models, limiting their applicability. Although we were unable to monitor the therapeutic effect of the CAAR T cells, we did show that the CAAR T cells could selectively lyse target cells, reduce autoantibody titers, and result in a lower human platelet clearance rate (*Online Supplementary Figure S4D*) in an *in vivo* xenograft mouse model. In addition, control of the anti-GPIb $\alpha$  hybridoma burden in LBD-mutg233k T-treated mice validated CAAR T-cell persistence *in vivo*. In order to verify the potential of GPIb $\alpha$  CAAR T cells in clinical applications, we first demonstrated their reactivity with sera from ITP patients with anti-GPIb antibodies. We found that anti-GPIb antibodies from patient 3 could bind to the LBD of GPIb $\alpha$  (LBD-mutg233k-CAAR) but did not react with CAAR3-mutg233k-CAAR or CAAR4-mutg233k-CAAR, which also contained the LBD. We hypothesized that the expression of the LBD is more stable than that of other extracellular domains of GPIb $\alpha$ , as it can mediate rapid downstream action.<sup>29</sup> In addition, studies have shown that the macroglycopeptide domain can affect the binding of LBD to ligands.<sup>44-46</sup> We anticipated that

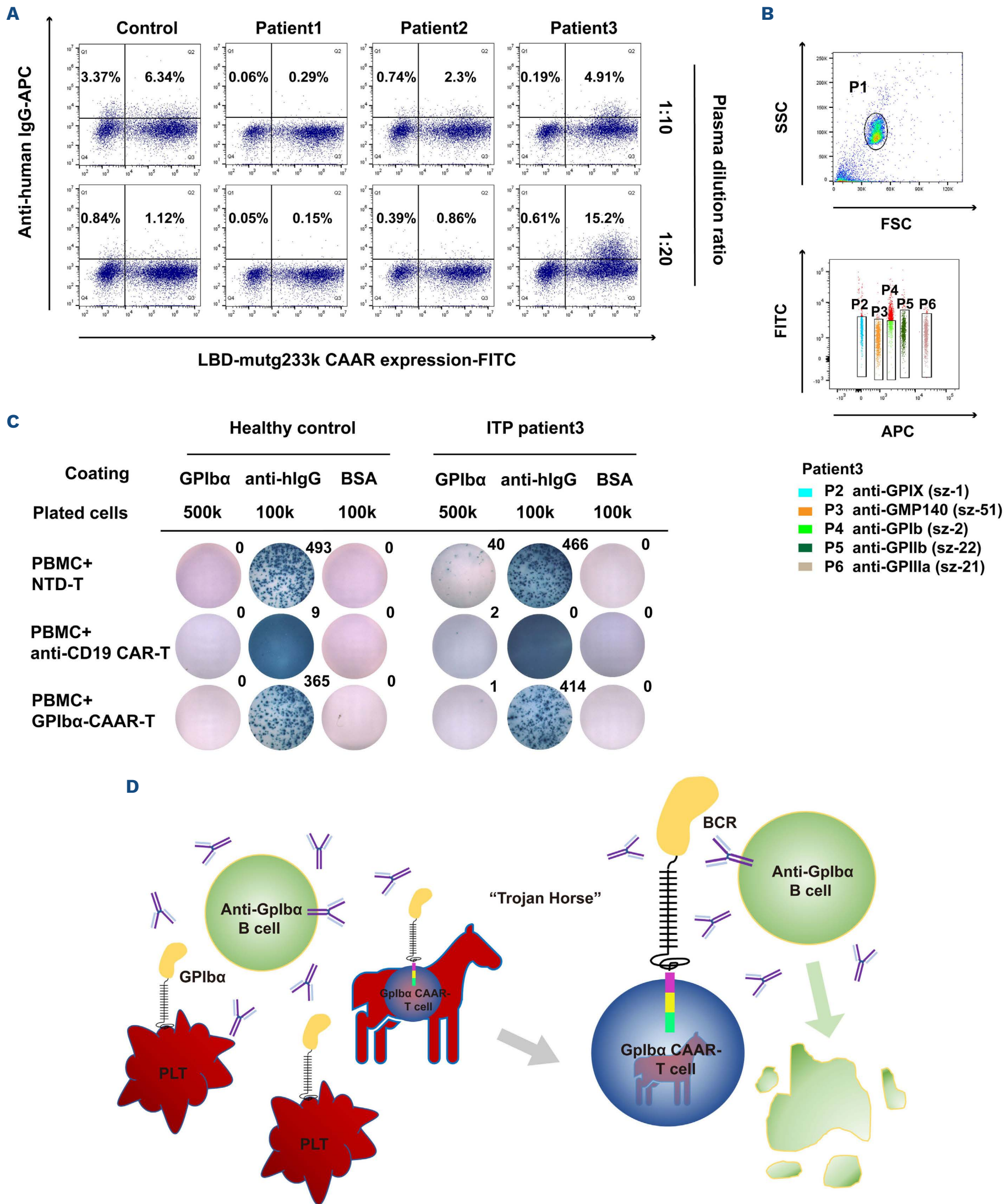


**Figure 6. GPIb $\alpha$  chimeric autoantibody receptor T cells recognized and eliminated autoreactive B cells from immune thrombocytopenia patients.** (A) Plasma from 3 immune thrombocytopenia (ITP) patients with anti-GPIb antibodies and healthy controls was diluted at 1:10 and 1:20 and incubated with HEK293T cells expressing ligand-binding domain LBD-mutg233k-chimeric autoantibody receptor (CAAR)-tagged with green fluorescent protein (GFP). The cells were then stained with anti-human immuno-

globulin (Ig)G antibodies (APC). (B) A cytometric bead array was applied to detect platelet-specific antibodies in ITP patient 3. Cutoff values were determined with reference to negative controls (mean + 3 standard deviations). Autoantibodies targeting human platelet GPIX/GPIb/GPIIb/GPIIIa/GMP140 were detected. GMP140, granule membrane protein 140. (C) Peripheral blood mononuclear cells (PBMC) from ITP patient 3 or healthy controls were stimulated with interleukin (IL)-2 and R848 for 2 days and then co-cultured with GPIb $\alpha$  CAAR T, anti-CD19CAR T, or non-transduced T (NTD T) cells for 1 day on plates coated with GPIb $\alpha$  protein and anti-human IgG antibody. Bovine serum albumin (BSA) served as a negative control antigen. One spot represents IgG antibodies secreted by a single B cell. The number of spots detected in each well is shown in the top right corner. (D) The conceptual graph of GPIb $\alpha$  CAAR T therapy in ITP. GPIb $\alpha$  CAAR T cells act like a “Trojan horse”, trapping autoreactive B cells and performing specific killing. PLT: platelet; BCR: B-cell receptor.

macroglycopeptide sequences could form large steric hindrances, interfering with antibodies' binding to CAAR structures (CAAR3-mutg233k-CAAR and CAAR4-mutg233k-CAAR). Furthermore, the structure of MSD is unstable,<sup>28</sup> and we can't tell whether the MSD expressed in the CAAR structure is folded or expanded, which may also interfere with the binding of CAAR3-mutg233k-CAAR and autoantibodies. The changes that occurred in the O-glycosylated macroglycopeptide domain and MSD in the CAAR expressed in the cells are worth exploring. An exciting and gratifying result was that GPIb $\alpha$  CAAR T cells successfully eliminated anti-GPIb $\alpha$  B cells from a patient with refractory ITP, and normal B cells were not destroyed compared to anti-CD19 CAR T cells, supporting further clinical application.

As anti-GPIIb/IIIa( $\alpha$ IIb/ $\beta$ 3)<sup>5,47</sup> is the most commonly detected autoantibody in ITP patients, we are also trying to construct GPIIb/IIIa-CAAR T cells. However, platelet-associated anti-GPIIb/IIIa autoantibodies from chronic ITP patients mainly depend on conformationally intact GPIIb/IIIa and divalent cations for maximal binding.<sup>5,48</sup> The N-terminal globular head of GPIIb-IIIa seems to play an essential role as a hot spot for autoantigenic epitopes in chronic ITP.<sup>49</sup> Integrating both  $\alpha$ IIb and  $\beta$ 3 into the CAAR structure is difficult, and it is challenging to ensure that the conformational epitopes created by the two subunits are consistent with the native epitopes. Though difficult, related work is still being done by our team. In summary, a novel GPIb $\alpha$  CAAR was constructed, and we demonstrated GPIb $\alpha$  CAAR T-cell's efficacy and safety *in vitro* and *in vivo* models. GPIb $\alpha$  CAAR T-cell therapy is a

viable treatment option for patients with refractory and relapsed ITP.

### Disclosures

No conflicts of interest to disclose.

### Contributions

HM, JL, JZ and YX designed the experiments. HM, JL and YH analyzed the data. ZJ and HM wrote the paper. JZ and YX performed the experiments. JS, HJ, LH and MX helped with the experiments.

### Acknowledgments

The authors thank Jun Peng and Ming Hou from Qilu Hospital, Shandong University, for providing specimens and for their helpful comments and suggestions.

### Funding

This work was supported by the National Natural Science Foundation of China (grant 82070124 to HM, and grant 82330005 to HM), the Technology Innovation Plan key research and development projects of Hubei Province (grant 2023BCB019 to HM), and the Basic Research Support Programs Foundation of Huazhong University of Science and Technology (grant 2023BR033 to HM).

### Data-sharing statement

Data that support the findings of this study are available from the corresponding author upon reasonable request.

## References

- Cooper N, Ghanima W. Immune thrombocytopenia. *N Engl J Med*. 2019;381(10):945-955.
- Stockelberg D, Hou M, Jacobsson S, Kutti J, Wadenvik H. Evidence for a light chain restriction of glycoprotein Ib/IX and IIb/IIIa reactive antibodies in chronic idiopathic thrombocytopenic purpura (ITP). *Br J Haematol*. 1995;90(1):175-179.
- Roark JH, Bussel JB, Cines DB, Siegel DL. Genetic analysis of autoantibodies in idiopathic thrombocytopenic purpura reveals evidence of clonal expansion and somatic mutation. *Blood*. 2002;100(4):1388-1398.
- Hou M, Stockelberg D, Kutti J, Wadenvik H. Immunoglobulins targeting both GPIIb/IIIa and GPIb/IX in chronic idiopathic thrombocytopenic purpura (ITP): evidence for at least two different IgG antibodies. *Br J Haematol*. 1997;98(1):64-67.
- McMillan R. Autoantibodies and autoantigens in chronic immune thrombocytopenic purpura. *Semin Hematol*. 2000;37(3):239-248.
- Arnold DM, Dentali F, Crowther MA, et al. Systematic review: efficacy and safety of rituximab for adults with idiopathic thrombocytopenic purpura. *Ann Intern Med*. 2007;146(1):25-33.
- Deshayes S, Khellaf M, Zarour A, et al. Long-term safety and efficacy of rituximab in 248 adults with immune thrombocytopenia: results at 5 years from the French prospective registry ITP-ritux. *Am J Hematol*. 2019;94(12):1314-1324.
- Tjønnfjord E, Holme PA, Darne B, et al. Long-term outcomes of patients treated with rituximab as second-line treatment for adult immune thrombocytopenia - follow-up of the RITP study. *Br J Haematol*. 2020;191(3):460-465.
- Canales-Herrerias P, Crickx E, Broketa M, et al. High-affinity autoreactive plasma cells disseminate through multiple organs

- in patients with immune thrombocytopenic purpura. *J Clin Invest.* 2022;132(12):e153580.
10. Yu TS, Wang HY, Zhao YJ, et al. Abnormalities of bone marrow B cells and plasma cells in primary immune thrombocytopenia. *Blood Adv.* 2021;5(20):4087-4101.
  11. Mahévas M, Patin P, Huetz F, et al. B cell depletion in immune thrombocytopenia reveals splenic long-lived plasma cells. *J Clin Invest.* 2013;123(1):432-442.
  12. Crickx E, Chappert P, Sokal A, et al. Rituximab-resistant splenic memory B cells and newly engaged naive B cells fuel relapses in patients with immune thrombocytopenia. *Sci Transl Med.* 2021;13(589):eabc3961.
  13. Kuwana M, Okazaki Y, Kaburaki J, Kawakami Y, Ikeda Y. Spleen is a primary site for activation of platelet-reactive T and B cells in patients with immune thrombocytopenic purpura. *J Immunol.* 2002;168(7):3675-3682.
  14. Ellebrecht CT, Bhoj VG, Nace A, et al. Reengineering chimeric antigen receptor T cells for targeted therapy of autoimmune disease. *Science.* 2016;353(6295):179-184.
  15. Oh S, Mao X, Manfredo-Vieira S, et al. Precision targeting of autoantigen-specific B cells in muscle-specific tyrosine kinase myasthenia gravis with chimeric autoantibody receptor T cells. *Nat Biotechnol.* 2023;41(9):1229-1238.
  16. Kroll MH, Harris TS, Moake JL, Handin RI, Schafer AI. von Willebrand factor binding to platelet GpIb initiates signals for platelet activation. *J Clin Invest.* 1991;88(5):1568-1573.
  17. Du X. Signaling and regulation of the platelet glycoprotein Ib-IX-V complex. *Curr Opin Hematol.* 2007;14(3):262-269.
  18. Nomura S, Yanabu M, Soga T, et al. Analysis of idiopathic thrombocytopenic purpura patients with antiglycoprotein IIb/IIIa or Ib autoantibodies. *Acta Haematol.* 1991;86(1):25-30.
  19. Hou M, Stockelberg D, Kutti J, Wadenvik H. Antibodies against platelet GPIb/IX, GPIIb/IIIa, and other platelet antigens in chronic idiopathic thrombocytopenic purpura. *Eur J Haematol.* 1995;55(5):307-314.
  20. Peng J, Ma SH, Liu J, et al. Association of autoantibody specificity and response to intravenous immunoglobulin G therapy in immune thrombocytopenia: a multicenter cohort study. *J Thromb Haemost.* 2014;12(4):497-504.
  21. Go RS, Johnston KL, Bruden KC. The association between platelet autoantibody specificity and response to intravenous immunoglobulin G in the treatment of patients with immune thrombocytopenia. *Haematologica.* 2007;92(2):283-284.
  22. Feng R, Liu X, Zhao Y, et al. GPIIb/IIIa autoantibody predicts better rituximab response in ITP. *Br J Haematol.* 2018;182(2):305-307.
  23. Webster ML, Sayeh E, Crow M, et al. Relative efficacy of intravenous immunoglobulin G in ameliorating thrombocytopenia induced by antiplatelet GPIIb/IIIa versus GPIIb/IIIa antibodies. *Blood.* 2006;108(3):943-946.
  24. Yu Y, Hou Y, Zhao Y, et al. Platelet autoantibody specificity and response to rhTPO treatment in patients with primary immune thrombocytopenia. *Br J Haematol.* 2021;194(1):191-194.
  25. He R, Reid DM, Jones CE, Shulman NR. Extracellular epitopes of platelet glycoprotein Ib alpha reactive with serum antibodies from patients with chronic idiopathic thrombocytopenic purpura. *Blood.* 1995;86(10):3789-3796.
  26. Nieswandt B, Bergmeier W, Rackebrandt K, Gessner JE, Zirngibl H. Identification of critical antigen-specific mechanisms in the development of immune thrombocytopenic purpura in mice. *Blood.* 2000;96(7):2520-2527.
  27. Jayaraman J, Mellody MP, Hou AJ, et al. CAR-T design: elements and their synergistic function. *EBioMedicine.* 2020;58:102931.
  28. Zhang W, Deng W, Zhou L, et al. Identification of a juxtamembrane mechanosensitive domain in the platelet mechanosensor glycoprotein Ib-IX complex. *Blood.* 2015;125(3):562-569.
  29. Quach ME, Dragovich MA, Chen W, et al. Fc-independent immune thrombocytopenia via mechanomolecular signaling in platelets. *Blood.* 2013;121(7):787-796.
  30. Xu M, Li J, Neves MAD, et al. GPIIb/IIIa is required for platelet-mediated hepatic thrombopoietin generation. *Blood.* 2018;132(6):622-634.
  31. Huizinga EG, Tsuji S, Romijn RA, et al. Structures of glycoprotein Ibalpha and its complex with von Willebrand factor A1 domain. *Science.* 2002;297(5584):1176-1179.
  32. Matsubara Y, Murata M, Sugita K, Ikeda Y. Identification of a novel point mutation in platelet glycoprotein Ibalpha, Gly to Ser at residue 233, in a Japanese family with platelet-type von Willebrand disease. *J Thromb Haemost.* 2003;1(10):2198-2205.
  33. Dong J, Schade AJ, Romo GM, et al. Novel gain-of-function mutations of platelet glycoprotein Ibalpha by valine mutagenesis in the Cys209-Cys248 disulfide loop. Functional analysis under static and dynamic conditions. *J Biol Chem.* 2000;275(36):27663-27670.
  34. Li J, van der Wal DE, Zhu G, et al. Desialylation is a mechanism of Fc-independent platelet clearance and a therapeutic target in immune thrombocytopenia. *Nat Commun.* 2015;6:7737.
  35. Tao L, Zeng Q, Li J, et al. Platelet desialylation correlates with efficacy of first-line therapies for immune thrombocytopenia. *J Hematol Oncol.* 2017;10(1):46.
  36. Kosugi S, Kurata Y, Tomiyama Y, et al. Circulating thrombopoietin level in chronic immune thrombocytopenic purpura. *Br J Haematol.* 1996;93(3):704-706.
  37. Guo L, Kapur R, Aslam R, et al. CD20+ B-cell depletion therapy suppresses murine CD8+ T-cell-mediated immune thrombocytopenia. *Blood.* 2016;127(6):735-738.
  38. Audia S, Rossato M, Trad M, et al. B cell depleting therapy regulates splenic and circulating T follicular helper cells in immune thrombocytopenia. *J Autoimmun.* 2017;77:89-95.
  39. Li J, Callum JL, Lin Y, Zhou Y, Zhu G, Ni H. Severe platelet desialylation in a patient with glycoprotein Ib/IX antibody-mediated immune thrombocytopenia and fatal pulmonary hemorrhage. *Haematologica.* 2014;99(4):e61-63.
  40. Xiao Q, Zhang X, Tu L, Cao J, Hinrichs CS, Su X. Size-dependent activation of CAR-T cells. *Sci Immunol.* 2022;7(74):eabl3995.
  41. Leick MB, Silva H, Scarfò I, et al. Non-cleavable hinge enhances avidity and expansion of CAR-T cells for acute myeloid leukemia. *Cancer Cell.* 2022;40(5):494-508.
  42. Lan P, Tonomura N, Shimizu A, Wang S, Yang YG. Reconstitution of a functional human immune system in immunodeficient mice through combined human fetal thymus/liver and CD34+ cell transplantation. *Blood.* 2006;108(2):487-492.
  43. Hu Z, Yang YG. Full reconstitution of human platelets in humanized mice after macrophage depletion. *Blood.* 2012;120(8):1713-1716.
  44. Othman M, Notley C, Lavender FL, et al. Identification and functional characterization of a novel 27-bp deletion in the macroglycopeptide-coding region of the GPIBA gene resulting in platelet-type von Willebrand disease. *Blood.* 2005;105(11):4330-4336.
  45. López JA, Ludwig EH, McCarthy BJ. Polymorphism of human glycoprotein Ib alpha results from a variable number of tandem repeats of a 13-amino acid sequence in the mucin-like macroglycopeptide region. Structure/function implications. *J Biol Chem.* 1992;267(14):10055-10061.

46. Li CQ, Dong JF, López JA. The mucin-like macroglycopeptide region of glycoprotein Ibalpha is required for cell adhesion to immobilized von Willebrand factor (VWF) under flow but not for static VWF binding. *Thromb Haemost.* 2002;88(4):673-677.
47. Brighton TA, Evans S, Castaldi PA, Chesterman CN, Chong BH. Prospective evaluation of the clinical usefulness of an antigen-specific assay (MAIPA) in idiopathic thrombocytopenic purpura and other immune thrombocytopenias. *Blood.* 1996;88(1):194-201.
48. Fujisawa K, Tani P, McMillan R. Platelet-associated antibody to glycoprotein IIb/IIIa from chronic immune thrombocytopenic purpura patients often binds to divalent cation-dependent antigens. *Blood.* 1993;81(5):1284-1289.
49. Tomiyama Y, Kosugi S. Autoantigenic epitopes on platelet glycoproteins. *Int J Hematol.* 2005;81(2):100-105.